Beam energy scan in a UrQMD+hydro hybrid model

J. Auvinen
(in collaboration with H. Petersen)

Frankfurt Institute for Advanced Studies
Germany

Transport meeting
April 25, 2013

Outline

Beam energy scan

First order phase transition with critical point?

QGP volume and lifetime decreases with decreasing $\sqrt{s_{NN}} \Rightarrow$ completely vanishes at some point?

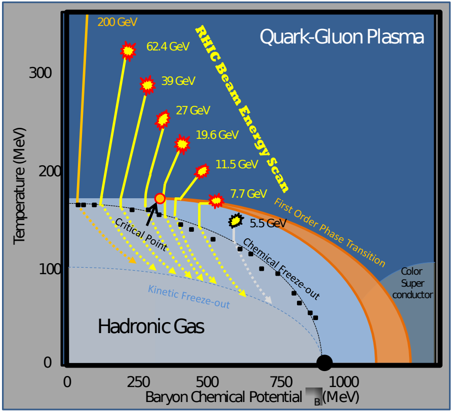

Picture taken from G. Odyniec, Acta Phys. Polon. B 43, 627 (2012).

Beam energy scan

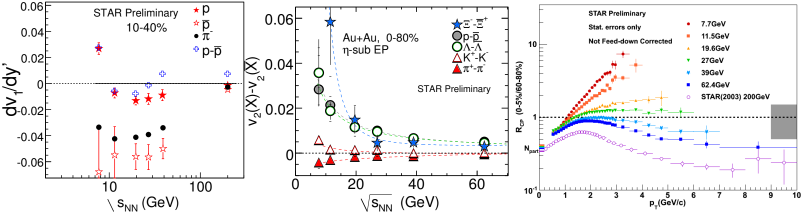

Some interesting findings:

- Non-monotonic $\sqrt{s_{NN}}$ dependence of net-proton v_1
- Difference in particle and antiparticle v_2 at lower energies
- R_{CP} suppression turns to enhancement between $\sqrt{s_{NN}} = 39$ and 27 GeV

v_1 and v_2 figures from L. Kumar [STAR Collaboration], arXiv:1211.1350 [nucl-ex],

R_{CP} from Hot Quarks 2012 talk by S. Horvat.

Beam energy scan

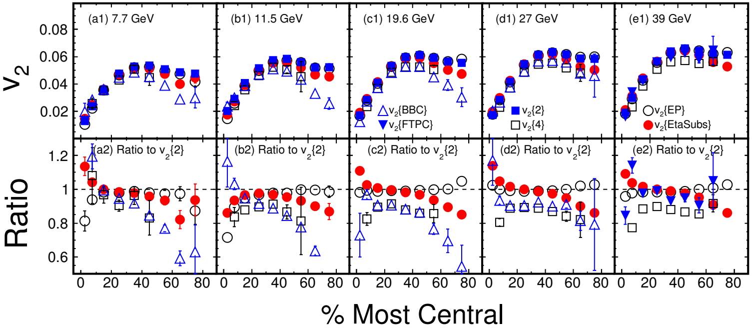

Charged hadron v_2 shows weak collision energy dependence.

L. Adamczyk *et al.* [STAR Collaboration], Phys. Rev. C 86, 054908 (2012).

Beam energy scan

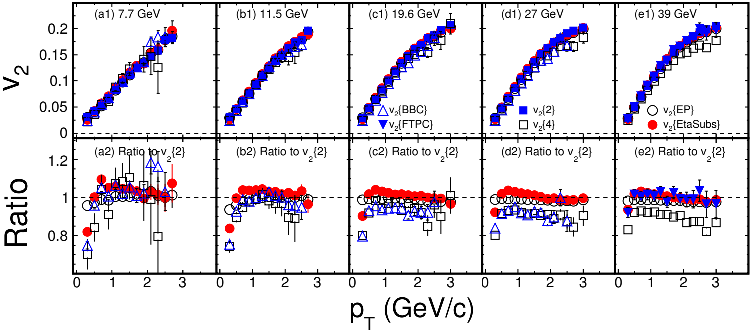

Differential v_2 almost identical for all $\sqrt{s_{NN}}$.

L. Adamczyk *et al.* [STAR Collaboration], Phys. Rev. C 86, 054908 (2012).

Beam energy scan

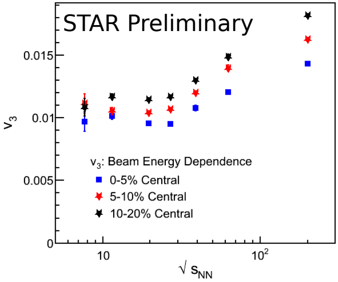

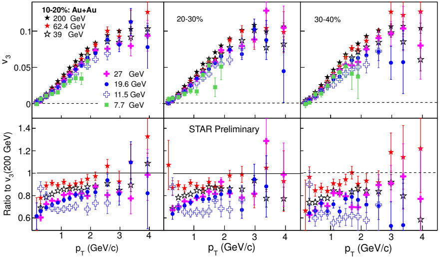

v_3 more sensitive to beam energy?

Y. Pandit [STAR Collaboration], QM2012 talk; arXiv:1210.5315.

Hybrid model

Transport + hydrodynamics hybrid model

H. Petersen, J. Steinheimer, G. Burau, M. Bleicher and H. Stocker, Phys. Rev. C 78, 044901 (2008).

Initial State from UrQMD[1] string/hadronic cascade

- Start the hydrodynamical evolution when nuclei have passed through each other: $t_{\text{start}} = \max\{\frac{2R_{\text{nuclei}}}{\sqrt{\gamma_{CM}^2 - 1}}, 0.5\text{ fm}\}$.
- Energy-, momentum- and baryon number densities (3D Gaussians) are mapped onto the hydro grid
- Event-by-event fluctuations are taken into account (width of Gaussians $\sigma = 1.0$ fm.)
- Spectators are propagated separately in the cascade

[1] S. A. Bass *et al.*, Prog. Part. Nucl. Phys. 41, 255 (1998), M. Bleicher *et al.*, J. Phys. G 25, 1859 (1999).

Hydro starting times

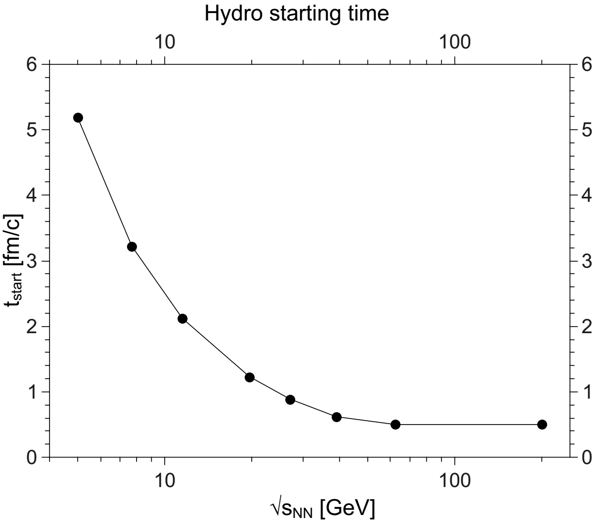

Transport + hydrodynamics hybrid model

H. Petersen, J. Steinheimer, G. Burau, M. Bleicher and H. Stocker, Phys. Rev. C **78**, 044901 (2008).

Hydrodynamical evolution

- (3+1)D ideal hydrodynamics using SHASTA[2]
- Equation of state[3]:
  - Chiral model coupled to Polyakov loop to include the deconfinement phase transition
  - Qualitative agreement with lattice QCD data at $\mu_B = 0$
  - Applicable also at finite baryon densities
  - Has the same degrees of freedom as UrQMD in hadronic phase

[2] D. H. Rischke, S. Bernard and J. A. Maruhn, Nucl. Phys. A **595**, 346 (1995), D. H. Rischke, Y. Pursun and J. A. Maruhn, Nucl. Phys. A **595**, 383 (1995).

[3] J. Steinheimer, S. Schramm and H. Stocker, J. Phys. G **38**, 035001 (2011).

Hydro duration in computational frame

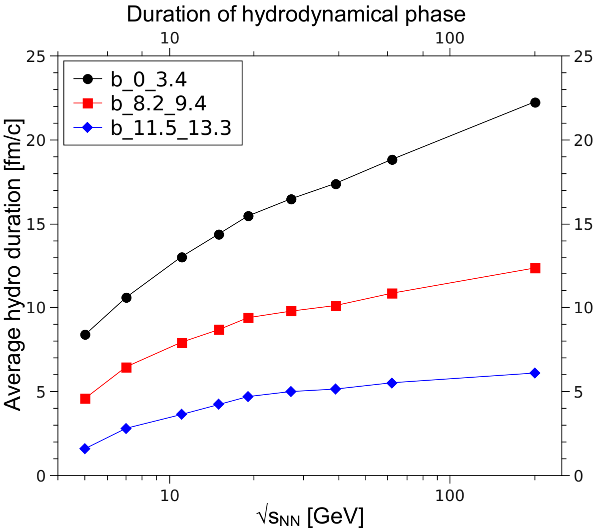

Transport + hydrodynamics hybrid model

H. Petersen, J. Steinheimer, G. Burau, M. Bleicher and H. Stocker, Phys. Rev. C 78, 044901 (2008).

Freeze-out Procedure

- Transition from hydro to transport ("particlization") when energy density ϵ is smaller than critical value $x\epsilon_0$, where $\epsilon_0 = 146$ MeV/fm^3 represents the nuclear ground state and $x \geq 1$.[4]
- Particle distributions are generated according to the Cooper-Frye formula
- Rescatterings and final decays calculated via hadronic cascade (UrQMD)

[4] In this study $x = 2$, corresponding to temperature $T \approx 154$ MeV.

Transport + hydrodynamics hybrid model

Cornelius hypersurface finding algorithm

P. Huovinen and H. Petersen, arXiv:1206.3371.

A method for finding the elements of 3D particlization hypersurface in 4D space for the Cooper-Frye procedure, without holes or double counting

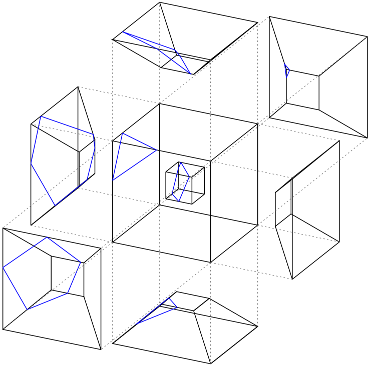

Fig. 9. Reduction of a four dimensional problem into a series of three dimensional problems.

Results

Particle multiplicity

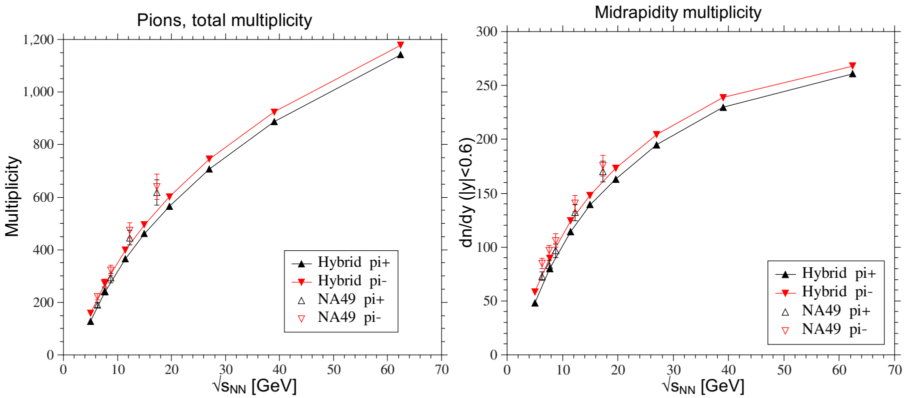

Charged pion multiplicity as a function of $\sqrt{s_{NN}}$.

Particle multiplicity

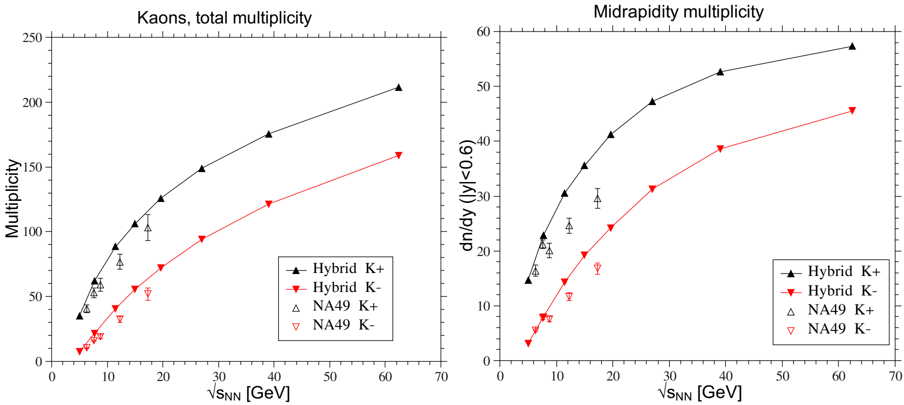

Charged kaon multiplicity as a function of $\sqrt{s_{NN}}$.

Particle m_T spectra

(0-7)% centrality.

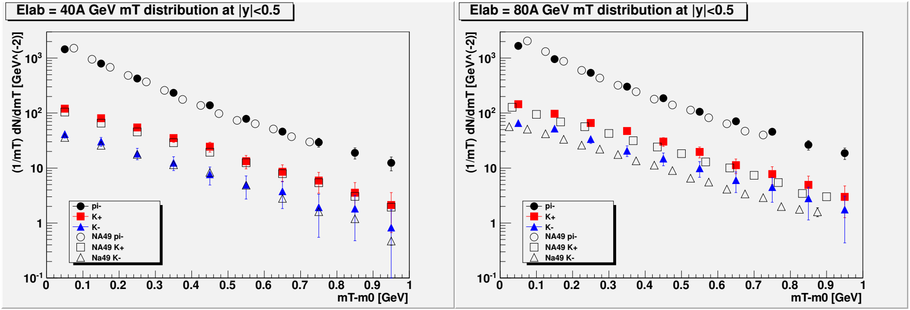

Left: π^-, K^+, K^- at $\sqrt{s_{NN}} \approx 9$ GeV.
Right: π^-, K^+, K^- at $\sqrt{s_{NN}} \approx 12$ GeV.

S. V. Afanasiev *et al.* [NA49 Collaboration], Phys. Rev. C **66**, 054902 (2002).

Particle m_T spectra

(0-7)% centrality. (0-5)% centrality.

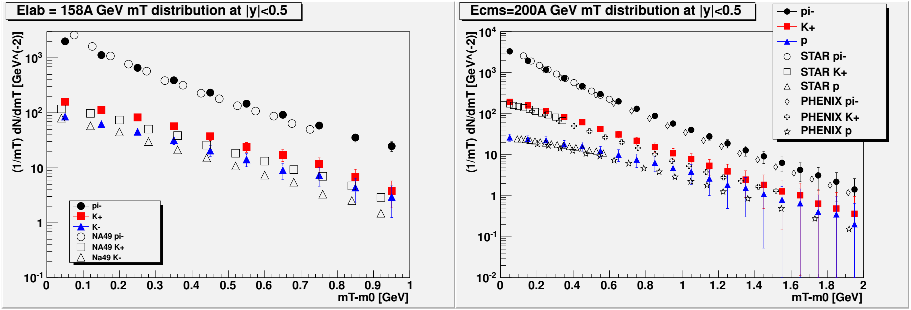

Left: π^-, K^+, K^- at $\sqrt{s_{NN}} \approx 17$ GeV.
Right: π^-, K^+, p at $\sqrt{s_{NN}} = 200$ GeV.

S. V. Afanasiev *et al.* [NA49 Collaboration], Phys. Rev. C 66, 054902 (2002).
J. Adams *et al.* [STAR Collaboration], Phys. Rev. Lett. 92, 112301 (2004),

S. S. Adler *et al.* [PHENIX Collaboration], Phys. Rev. C 69, 034909 (2004).

Elliptic flow

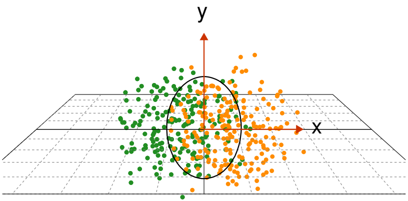

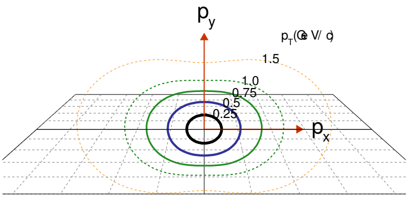

P. Sorensen, arXiv:0905.0174 [nucl-ex].

Initial spatial asymmetry: eccentricity $\epsilon_2 = \frac{\sqrt{\langle r^2\cos(2\phi)\rangle^2 + \langle r^2\sin(2\phi)\rangle^2}}{\langle r^2\rangle}$.

Final momentum anisotropy: $v_2\{\text{EP}\} = \frac{v_2\{\text{observed}\}}{R_2} = \frac{\langle\langle\cos[2(\phi_i - \psi_2)]\rangle\rangle}{\langle\cos[2(\psi_2 - \psi_2^{\text{true}})]\rangle}$

Elliptic flow

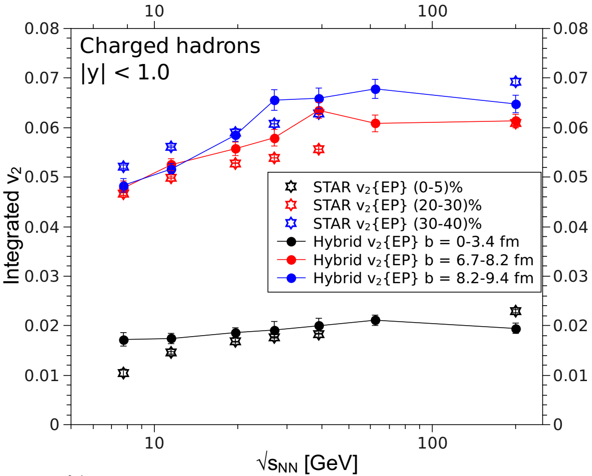

Rising slope in 0-5% centrality not reproduced; rough agreement at midcentrality.

L. Adamczyk *et al.* [STAR Collaboration], Phys. Rev. C 86, 054908 (2012).

Elliptic flow

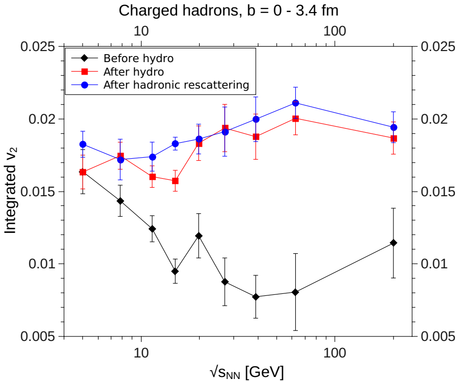

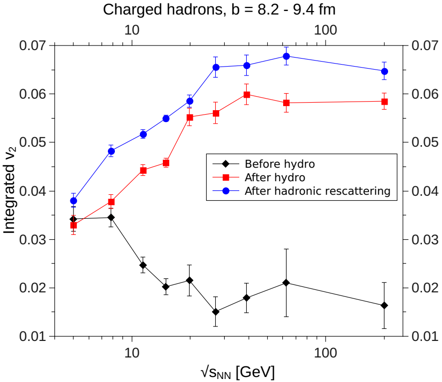

No contribution from hadronic rescattering in most central collisions.
Pre-equilibrium dynamics become more important at lower energies.

Hydro contribution on v_2

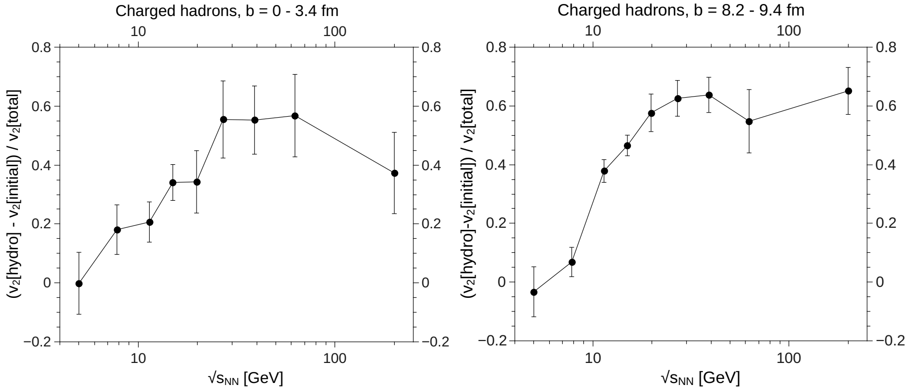

Hydro contribution to v_2 negligible at $\sqrt{s_{NN}} = 5$ GeV; roughly 60% at highest energies.

Elliptic flow

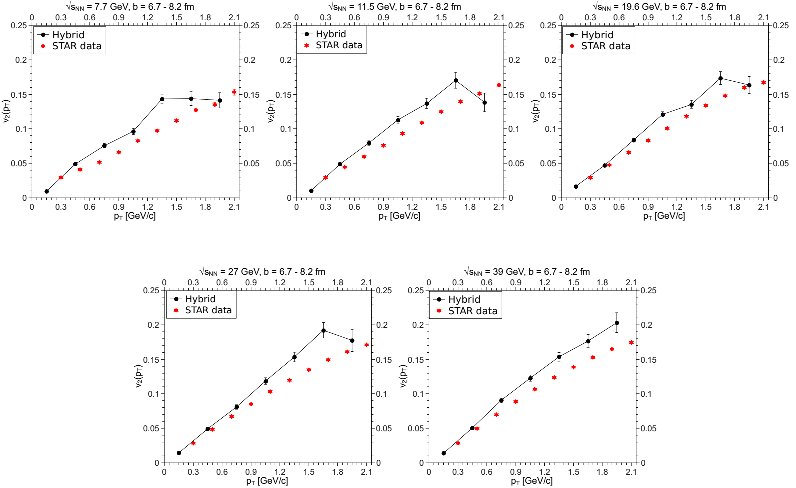

$v_2(p_T)$ overestimated at higher p_T.

L. Adamczyk *et al.* [STAR Collaboration], Phys. Rev. C **86**, 054908 (2012).

Effect of hydro ending condition on elliptic flow

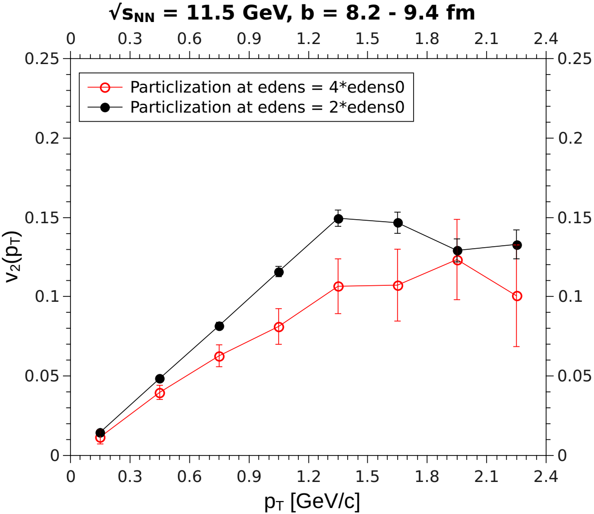

Revision of hydro-to-cascade transition condition could fix $v_2(p_T)$.

Elliptic flow

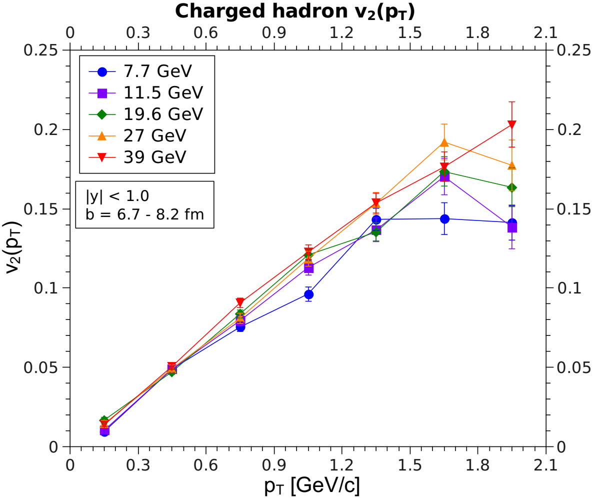

No clear energy dependence on differential flow.

Triangular flow

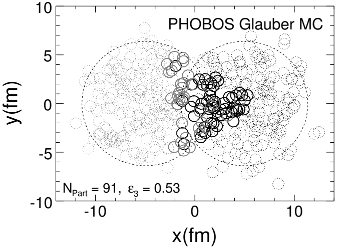

FIG. 3: Distribution of nucleons on the transverse plane for a $\sqrt{s_{NN}}$ = 200 GeV Au+Au collision event with ε_3=0.53 from Glauber Monte Carlo. The nucleons in the two nuclei are shown in gray and black. Wounded nucleons (participants) are indicated as solid circles, while spectators are dotted circles.

B. Alver and G. Roland, Phys. Rev. C 81, 054905 (2010), [arXiv:1003.0194].

Triangularity:

$$\epsilon_3 = \frac{\sqrt{\langle r^3 \cos(3\phi)\rangle^2 + \langle r^3 \sin(3\phi)\rangle^2}}{\langle r^3 \rangle}$$

$$v_3\{\mathrm{EP}\} = \frac{\langle\langle \cos[3(\phi_i - \psi_3)]\rangle\rangle}{\langle \cos[3(\psi_3 - \psi_3^{\mathrm{true}})]\rangle}$$

Triangular flow

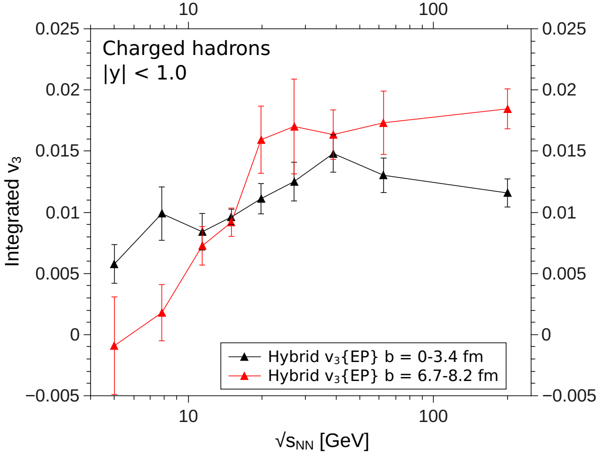

Midcentral v_3 rises from ≈ 0 to $\approx 0.015 - 0.02$.

Triangular flow

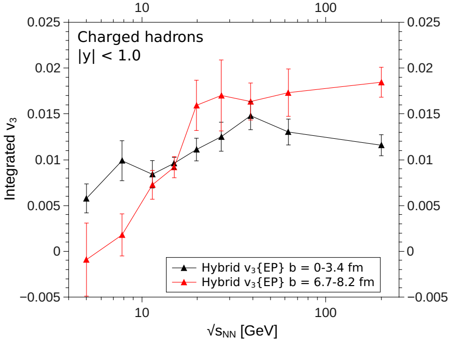

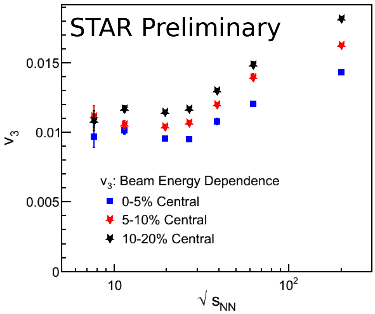

Preliminary data displays quite different behavior, however.

Y. Pandit [STAR Collaboration], QM2012 talk.

$v_3(p_T)$

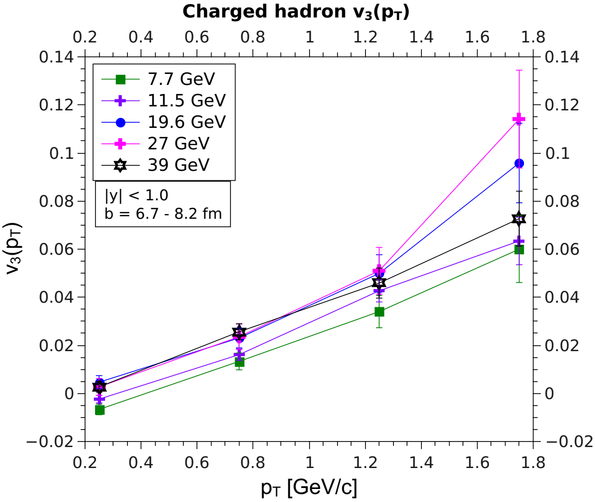

Increase at lower values of $\sqrt{s_{NN}}$; no change after 19.6 GeV.

$v_3(p_T)$

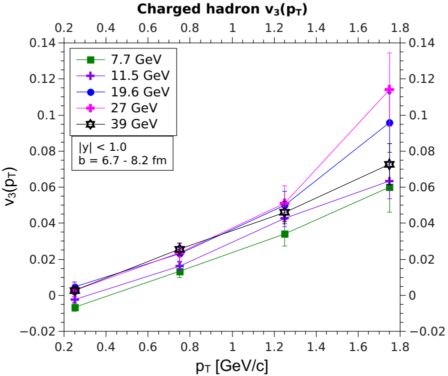

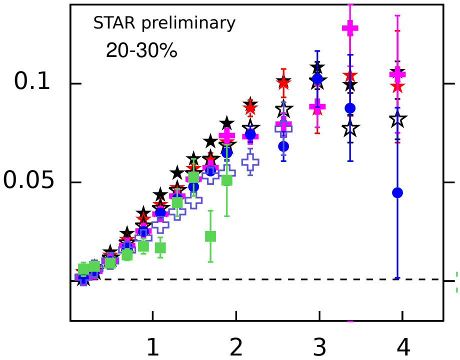

Comparison with preliminary STAR data.

Y. Pandit [STAR Collaboration], arXiv:1210.5315.

Collision geometry

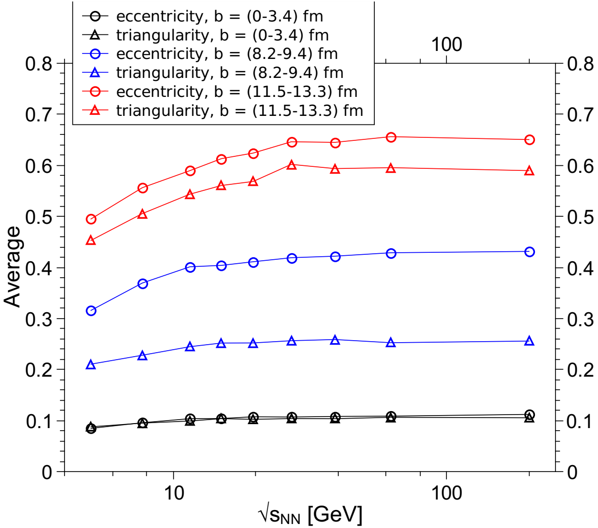

ϵ_2 more sensitive than ϵ_3 to changes on b and $\sqrt{s_{NN}}$.

Scaled flow coefficients

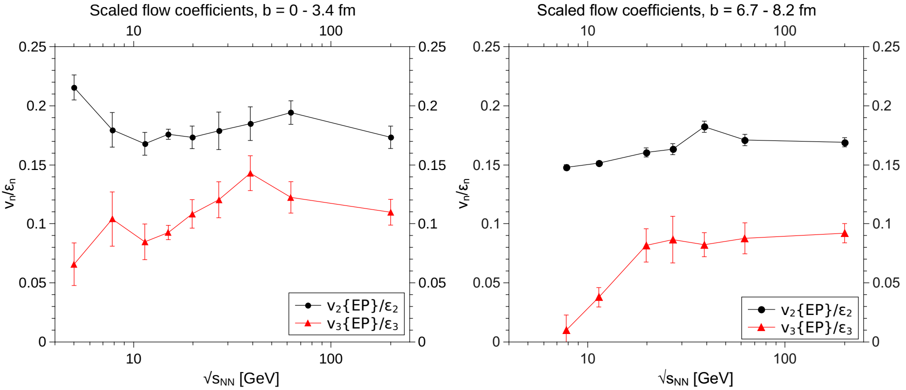

v_2 response to ϵ_2 remains roughly the same in both centrality classes and all energies.

Energy dependence of v_3 persists through scaling.

Summary

- Multiplicities: Pion production in reasonable agreement with data, kaons overproduced.
- Elliptic flow: Integrated v_2 similar to the STAR data, $v_2(p_T)$ overshoots the data (particlization at higher energy density?).
- Triangular flow: $v_3 \approx 0$ at $\sqrt{s_{NN}} = 5$ GeV, then rises until reaches value 0.015 - 0.02 at $\sqrt{s_{NN}}$ = 19.6 GeV.
  Qualitative disagreement with preliminary STAR data, which has flat v_3 at low $\sqrt{s_{NN}}$ and begins increasing at 27 GeV.

Extra slides

v_2 fluctuations

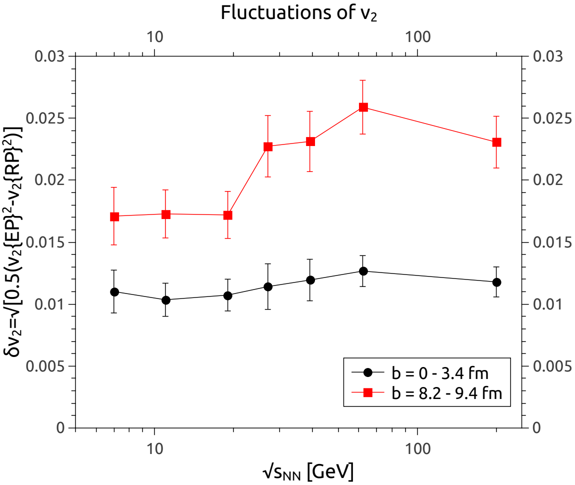

δv_2 visibly energy-dependent on midcentral collisions; equal to v_3 in magnitude in central collisions.

Eccentricity probability distributions

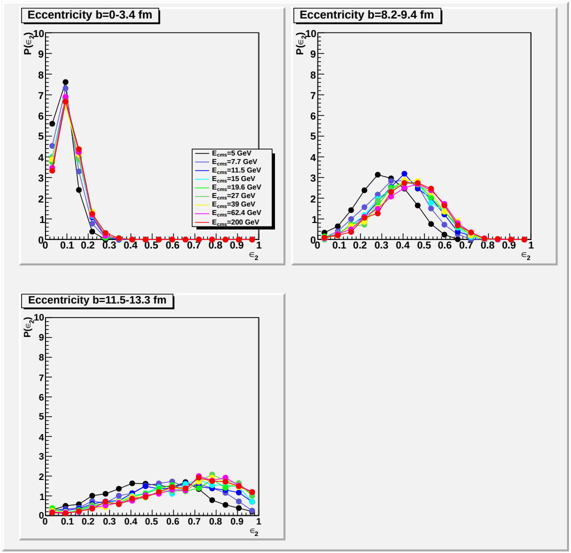

Triangularity probability distributions

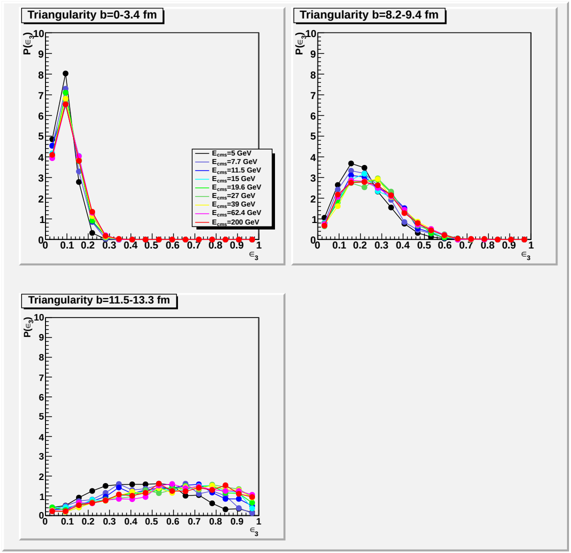

(Square root of) variances of $\langle\epsilon_2\rangle$ and $\langle\epsilon_3\rangle$

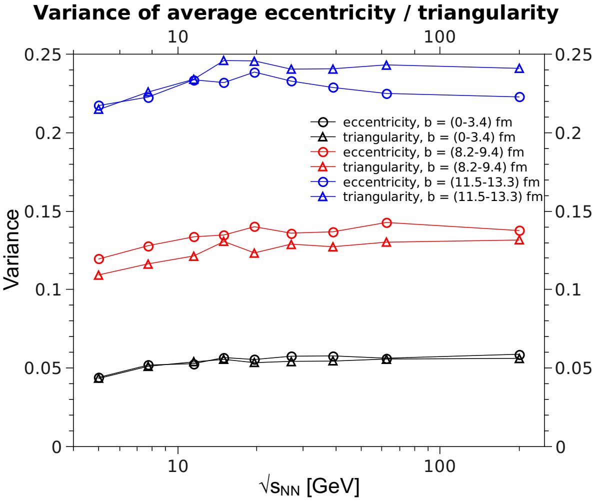

Both eccentricity and triangularity have variances of same size.

Relative variances of $\langle\epsilon_2\rangle$ and $\langle\epsilon_3\rangle$

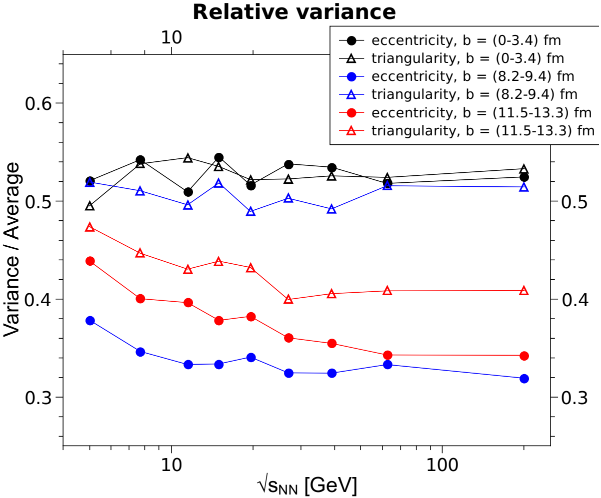

Triangularity has larger relative variance than eccentricity; remains practically same from most central to midcentral collisions.

Relative variance of $\langle\epsilon_2\rangle$ and v_2 fluctuations

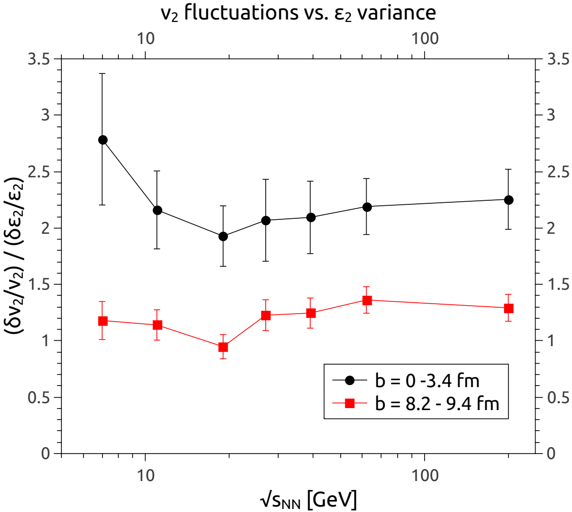

$\frac{\delta v_2}{v_2} \approx \frac{\delta \epsilon_2}{\epsilon_2}$ in midcentrality.

Energy-momentum tensor anisotropy

$$\epsilon_p = \frac{\langle T^{xx} - T^{yy} \rangle}{\langle T^{xx} + T^{yy} \rangle}$$